Optimal Power Flow for Combined AC and VSC-MTDC system with large penetration of wind farm

R. Kouadri
Department of Electrical Engineering
University of Ferhat Abbas Setif 1
Algeria.
ramzikouadri@gmail.com

L. Slimani
Department of Electrical Engineering
University of Ferhat Abbas Setif 1
Algeria
slimaniblinda@gmail.com

T. Bouktir
Department of Electrical Engineering
University of Ferhat Abbas Setif 1
Algeria
tarek.bouktir@esrgroups.org

***Abstract*-- In this paper, the optimal power flow (OPF) of a meshed AC/DC power transmission network with voltage source converter based multi-terminal DC (VSC-MTDC) networks has used to minimize the cost and the transmission losses. Furthermore, we have used the optimal power flow (OPF) in presence of VSC-MTDC with large integration of wind farm using the differential evolution (DE) method. Simulations are executed using MATACDC which is open source software for the analysis of hybrid AC/DC systems. The DE method has been tested on the standard IEEE 30 test system with different objectives that reflect active power losses minimizations and active power generation cost minimization.**

***Keywords* -- Optimal Power Flow (OPF), AC/DC, VSC, multi-terminal DC (MTDC), DE, MATACDC.**

1. INTRODUCTION

Multi-Terminal HVDC Grids (MTDC) based in the Voltage Source Converter (VSC) technology's gaining a lot of interest in the power system. The technology is considered more and more for future grid reinforcements and is currently being proposed as a technological candidate to build future offshore grids to interconnect offshore wind farms [1].

The Voltage Source Converter (VSC) technology's capabilities of multi-directional power flow and independent power control capability are fundamental to a MTDC grid system. With the systematic control of the VSCs and the MTDC grid system, the integration of wind farms and interconnections between countries can be made more reliable to support the AC network [2]. VSC based MTDC is considered to be a feasible solution for transmitting wind farm powers due to its significant advantages over both current source converter CSC, Line Commutated Converter (LCC) and traditional AC system [3].

Integrating wind farms by VSC-MTDC to power grid will inevitably present a big impact on the electrical system safety and economical operation of the system and such impact has become a lot research topic as wind farm power penetrations increase in power system in recent years [4].

By the use of optimal power flow (OPF) calculation we can find out the impact of wind farm energy with Multi-Terminal HVDC Grids on power system. The OPF is an important tool that system operators require in order to operate the grid with high penetration of wind farm power more efficiently with VSC-MTDC while maintaining all constraints within restricted limits [5].

The evolutionary algorithm for global optimization named it Differential Evolution (DE) was proposed by Storn and Price [6]. The Differential Evolution is characterized as a simple heuristic of well-balanced mechanism with flexibility to enhance and adapt to both global and local exploration abilities. The effectiveness, efficiency and robustness of the DE algorithm are sensitive to the settings of the control parameters [5].

The effect of optimal power flow for combined AC and VSC-MTDC system with connected to wind farm on the transmission grid has grown, as shown [7], [8], to minimized of the active losses, and as shown [9] to reduce the total generation cost.

This paper aim to study the optimal power flow for including wind farm by VSC-MTDC system. The differential evolution (DE) method is proposed to solve the optimal power flow problem. The proposed MTDC is building with voltage source converters (VSC) for transmission of wind farm power. The influence of the VSC-MTDC with large penetration of wind farm on the power systems are carried out on IEEE 30-bus test system. The objective function used is the minimization of the cost the thermal and the wind generators and the minimization the transmission losses. The results of simulation show that the optimal power flow of VSC-MTDC system with wind farms can reduce active losses, minimization of the cost the thermal and prevent overloads in electrical lines.

2. MODELING OF AC/MTDC SYSTEM

This section introduces the modeling of the AC/MTDC system. The modeling is based in the converter station and DC grids system models.

A. Converters

A general representation of a VSC-MTDC converter station, the different components is shown in Fig. 1. As seen from the AC point of common coupling (PCC), the different components are [10]:

- The converter transformer
- The AC filters
- The phase reactor
- The converter.

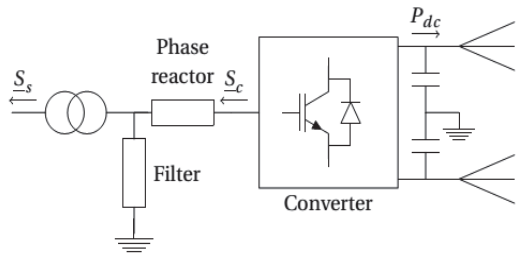

Fig. 1. VSC MTDC converter station [10]

1) AC side model

In the most general format, the AC side of the converter is represented as depicted in Fig. 2.

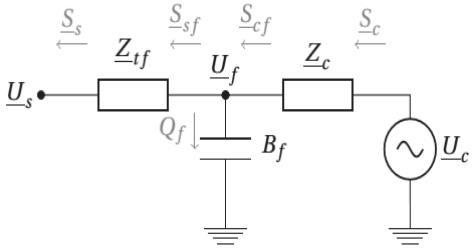

Fig. 2. Equivalent single phase power flow model of a converter station connected to the AC grid [10]

The model a converter station consists of a controllable voltage source $\underline{U_c} = U_c\angle\delta_c$behind the phase reactor, represented as complex impedance $\underline{Z_c} = R_c + jX_c$. the low pass filter from Fig. 2 is represented as a susceptance $B_f$at system frequencies. A transformer connects the filter bus to the AC grid and is represented by its complex impedance $\underline{Z_{tf}} = R_{tf} + jX_{tf}$[10].

The equations for active and reactive power at the grid side in terms of the complex voltages are:

$$P_S = -U_S^2 G_{tf} + U_s U_f\left[G_{tf}\cos(\delta_s - \delta_f) + B_{tf}\sin(\delta_s - \delta_f)\right] \quad (1)$$

$$Q_s = U_S^2 B_{tf} + B_s B_f\left[G_{tf}\sin(\delta_s - \delta_f) - B_{tf}\cos(\delta_s - \delta_f)\right] \quad (2)$$

With $\underline{U_s} = U_s\angle\delta_s$ and $\underline{U_f} = U_f\angle\delta_f$ respectively the complex grid side and filter bus voltage.
The equations at the converter side are:

$$P_c = U_c^2 G_c - U_f U_c\left[G_c\cos(\delta_f - \delta_c) - B_c\sin(\delta_f - \delta_c)\right] \quad (3)$$

$$Q_c = -U_c^2 B_c + U_f U_c\left[G_c\sin(\delta_f - \delta_c) + B_c\cos(\delta_f - \delta_c)\right] \quad (4)$$

The reactive power at the filter is given by

$$Q_f = -U_f^2 B_f \quad (5)$$

The expressions for the filter side complex power flowing through the transformer are written as

$$P_{sf} = U_f^2 G_{tf} - U_f U_s\left[G_{tf}\cos(\delta_s - \delta_f) - B_{tf}\sin(\delta_s - \delta_f)\right] \quad (6)$$

$$Q_{sf} = -U_f^2 B_{tf} + U_f U_s\left[G_{tf}\sin(\delta_s - \delta_f) + B_{tf}\cos(\delta_s - \delta_f)\right] \quad (7)$$

And those flowing through the phase reactor side are

$$P_{cf} = -U_f^2 G_c + U_f U_c\left[G_c\cos(\delta_f - \delta_c) + B_c\sin(\delta_f - \delta_c)\right] \quad (8)$$

$$Q_{cf} = U_f^2 B_c + U_f U_c\left[G_c\sin(\delta_f - \delta_c) - B_c\cos(\delta_f - \delta_c)\right] \quad (9)$$

2) Converter losses

Converter losses can be taken into account using a generalized loss formula quadratically depending on the convert current [11]:

$$P_{loss} = a + b.I_c + c.I_c^2 \quad (10)$$

The current I_c is given by the following expression:

$$I_c = \frac{\sqrt{P_c^2 + Q_c^2}}{\sqrt{3}U_c} \quad (11)$$

B. DC System modeling

The DC system modeling can be represented by a resistive network with current injections and DC voltages at the different nodes, as depicted in Fig.3 [12].

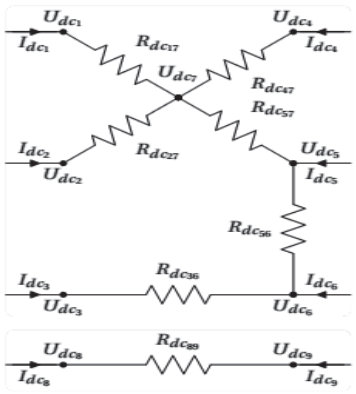

Fig. 3. DC grids modelling

The current injected at a DC node i can be written as the current flowing to the other n- 1 nodes in the network:

$$I_{dc_i} = \sum_{\substack{j=1 \\ j\neq 1}}^{n} Y_{dc_{ij}}.\left(U_{dc_i} - U_{dc_j}\right) \quad (12)$$

With $Y_{dc_{ij}}$ equal to $1/R_{dc_{ij}}$

The DC grid power flow equation can be written as

$$P_{dc_i} = pU_{dc_i}\sum_{\substack{j=1 \\ j\neq 1}}^{n} Y_{dc_{ij}}.\left(U_{dc_i} - U_{dc_j}\right) \quad (15)$$

With $Y_{dc_{ij}}$ equal to $1/R_{dc_{ij}}$ and p=1for a monopolair system or p=2 for a monopolair symmetrically grounded or bipolair system.

3. PROBLEM FORMULATION

A. Formulation of OPF

The standard OPF problem can be written in the following from:

$$MinF(x,u) \quad (14)$$

Subject to $g(x,u)=0$ (15)

$$h(x,u)\leq 0 \quad (16)$$

Where x the vector of state variables is, u is a vector of control variables, $f(x,u)$ is the objective function to be optimized, $h(x,u)$ represents the equality constraints, and $g(x,u)$ is the inequality constraints.

u: Vector of state variables includes the active power generated except the reference bus and power generated of the wind farms for the case for the incertion of the wind farms. The control vector is obtained by:

$$u^T=\left[P_{G2}\ldots.P_{NG},P_{GW_1}\ldots P_{GW_{nw}}\right] \quad (17)$$

B. Objectives Functions

In this paper, OPF is formulated with two objective functions as follows:

- *Minimization of cost of generation*

The OPF problem can be expressed as minimizing the cost of production of the real power which is given by a quadratic function of generator power output P_{Gi} as [13, 14].

$$F_1(x)=\sum_{i=1}^{ng}(A_i+B_iP_{Gi}+C_iP_{Gi}^2) \quad (18)$$

Where: F is the fuel cost function, A_i,B_i,C_i are the fuel cost coefficients, i represent the corresponding generator $(1,2,\ldots..ng)$, P_{Gi} is the generated active power at bus I and ng is number of generators including the slack bus.

- *Minimization of Transmission Loss*

The second objective function considered in the OPF model is the total active power loss.

$$F_2(x)=\sum_{k=1}^{L}g_{ij}\left(V_i^2+V_j^2-2V_iV_j\cos\theta_{ij}\right) \quad (19)$$

Where L is the number of the branches.

- *OPF constraints*

The constraints of the OPF problem can be split into two parts: The equality and inequality constraint [15]:

• The equality constraint is:

$$P_{g_i}-P_{d_i}=V_i\sum_{j=1}^{N}V_j\left(g_{ij}\cos\delta_{ij}+z_{ij}\sin\delta_{ij}\right) \quad (20)$$

$$Q_{g_i}-Q_{d_i}=V_i\sum_{j=1}^{N}V_j\left(g_{ij}\sin\delta_{ij}+z_{ij}\cos\delta_{ij}\right) \quad (21)$$

Where P_{G_i},Q_{G_i} are the active and the reactive power generation at bus i; P_{d_i},Q_{d_i} are the real and the reactive power demand at bus i, V_i,V_j the voltage magnitude at bus i, j, respectively g_{ij},z_{ij} are the real and imaginary part of the admittance (Y_{ij}); δ_{ij} is the phase angle difference between buses i and j respectively and N is the total number of buses.

• Constraints of inequality are:

- Limits on active power at generator buses

$$P_{Gi}^{min}\leq P_{Gi}\leq P_{Gi}^{max} \quad (22)$$

- the location constraint

$$N_{Li}^{min}\leq N_{Li}\leq N_L^{max} \quad (23)$$

- Limits on voltage magnitude of at the all buses

$$V_i^{min}\leq V_i\leq V_i^{max} \quad (24)$$

- Limits on transmission lines loading

$$|S_{Li}|\leq S_{Li}^{max} \quad (25)$$

C. Differential Evolution Optimization method

Differential Evolution (DE) is based on evolutionary behavior and was invented in 1995 by [16]. The main advantage of differential evolution (DE) is a high probability of finding the global optimum solution even when concerning complex nonlinear problems. Additionally Differential Evolution (DE) is capable of representing nonlinear and differential equation based problems which enable the algorithm for consideration of stability and security aspects in power systems including FACTS devices such as including HVDC in this paper [17].

Differential Evolution (DE) as all artificial intelligence optimization methods is based on crossover, mutation and selection of the most appropriate solutions as it is illustrated in Fig.4

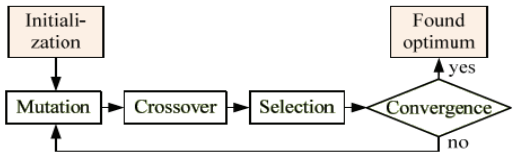

Fig. 4. Simplified Flowchart of DE Optimization

- *Initialization*

The population is initialized by randomly generating individuals (equation (27)) [18].

$$X_{ij}^0=X_j^{min}+rand*\left(X_j^{max}-X_j^{min}\right)$$

$$i=1,2,\ldots Np \ \ \& \ \ j=1,2,\ldots D \quad (26)$$

Where: the jth variable of the given problem has its lower X_j^{min} and upper X_j^{max} bound. Np is the size of the population and D is the number of decision variables.

- *Mutation*

The mutation operator of differential evolution occupies quite an important function in the reproduction cycle. This operation creates mutant vectors $X_j'^k$ by perturbing a randomly selected vector X_a^k with the difference of two other randomly selected vectors X_b^k and X_c^k at the th iteration equation (27) [19]:

$$X_i'^k = X_a^k + Fx * \left(X_b^k - X_c^k\right) \quad i = 1,2, \dots Np \qquad (27)$$

Where: Fx is the scaling factor, it used to control the amount of perturbation in the process (Fx ∈[0 2]).

- *Crossover*

Based on the mutant vector, the parent vector is mixed with the mutated vector to create a trial vector, which is used in the selection process according to the following equation:

$$X_{ij}''^k = \begin{cases} X_{ij}'^k & if\ rand\ j < Cr\ or\ j = randn \\ X_{ij}^k & otherwise \end{cases} \qquad (28)$$

Where: $i = 1, 2, 3, \dots, Np; j = 1, \dots, D$. $X_{ij}^k, X_{ij}'^k$ and $X_{ij}''^k$ are jth individual of ith target vector, mutant vector, and trial vector at kth iteration respectively. Cr ∈[0, 1] is the Crossover constant [20].

- *Selection*

Selection process is used among the set of trial vector and the updated target vector to choose the best. At last the fitness of the vector b and $X_i^k\ and X_i^{k+1}$ is compared, and the best is chosen to generate offspring through greedy selection, that is [19]:

$$X_I^{k+1} = \begin{cases} X_i''^k & if\ f\left(X_i''^k\right) \le f\left(X_i''^k\right) \\ X_i^k & otherwise \end{cases} \quad i = 1,2, Np \qquad (30)$$

4. RESULTS AND ANALYSIS

In this study, a four terminal MTDC system is integrated in the modified IEEE 30 bus system. The DC system voltage is +/- 132 kV. The converter station VSC1 (slack bus of the DC network) is connected to bus 10 and VSC3 is connected to bus 24 of the AC system. In addition the converter station VSC2 and VSC4 are connected with wind farms 1 and 2 respectively to capture maximum power from the two wind farms, as shown in Figure 5.The total load was 396.76 MW. Several scenarios with dispersed wind penetration levels from 5% to 30% of active total load have been investgated.

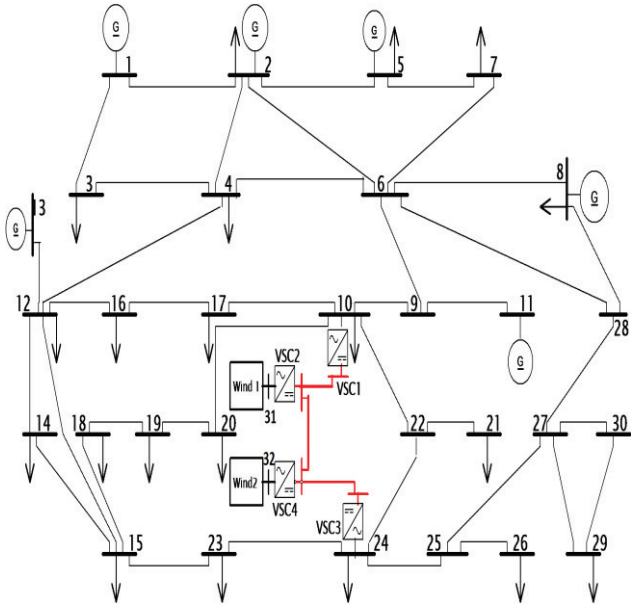

Fig.5 IEEE 30-bus system with VSC-MTDC networks and two Wind Farms

In this paper, the OPF-DE parameters are set as:

- Population size NP: 20.
- Maximum nbr of generations Gmax: 200.
- Crossover constant CR: 0.8.
- Weighting factor F: 0.8.
- Strategy: 1: DE/best/1/exp [21].

- *Simulation without VSC-MTDC and Wind Farms*

The results presented in Table I including the real power generation, generation cost and real power losses.

TABLE I

Resultants Simulation DE-OPF and PSO-OPF

Variables	min	max	DE-OPF	PSO-OPF
$P_{G1}(MW)$	50	200	200.00	200.00
$P_{G2}(MW)$	20	80	80.000	75.421
$P_{G5}(MW)$	15	50	32.067	36.672
$P_{G8}(MW)$	10	35	35.000	34.980
$P_{G11}(MW)$	10	30	30.000	30.000
$P_{G13}(MW)$	12	40	34.594	34.185
Active Loss MW	-	-	14.9010	14.4957
Cost ($/h)	-	-	1268.45	1270.4

The comparisons of the results obtained by the proposed approach DE, with those found by PSO algorithm are reported in the Table I. In this case, we minimized the fuel cost generation and total losses. The proposed approach shown better results for the cost generation; in contrary, the PSO has better value for the real power loss.

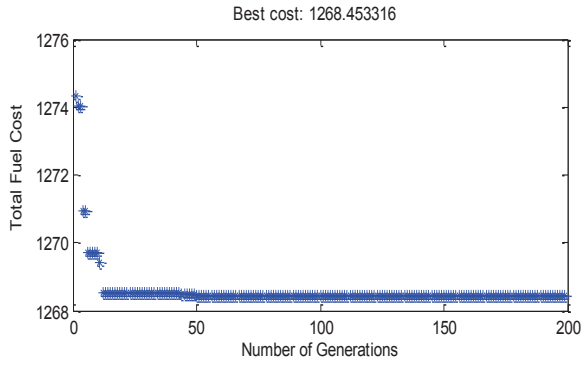

Fig.6 Convergence characteristic of the 6 generating units using DE

As shown Figure 7, the power transmitted in line 5 between buses 2 and 5 is 84.35 MW, and this value exceeded the maximum 80 MW.

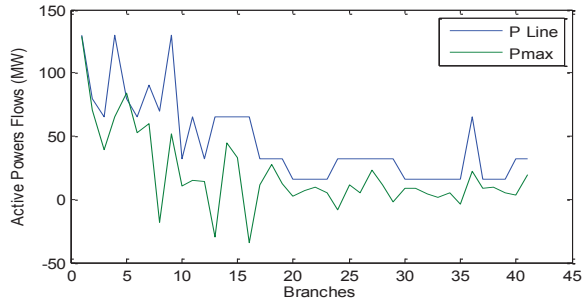

Fig.7 Active power transit in all branches

- *Simulation with VSC-MTDC and Wind Farms*

In this part we are going to study two different cases, the first one it's a multiple wind farm location and in the second we traid to see the effect of the outage of VSC4. The parameters and at the converter stations are given in Table II.

TABLE II

VSC Converter Data

Converter parameters		Rating & Converter loss data No.	1, 2,3,4
$X_{tr}(p.u)$	0.1121	$\pm V_{dc}$	132
$R_{tr}\ (p.u)$	0.0015		
$B_f\ (p.u)$	0.0887	a	1.103
$X_c\ (p.u)$	0.1642	b	0.887
$R_c\ (p.u)$	0.0001	c_{rec}	2.885
$R_{dc1-2}(p.u)$	0.0500	c_{inv}	4.371
$R_{dc3-4}(p.u)$	0.0400	$R_{dc2-4}(p.u)$	0.060

❖ **Case 1** : Multiple Wind Farm Location

In the multiple locations scenario, wind generation is connected to AC network simultaneously by using VSC-MTDC, and different penetration levels combinations were applied. Table III shows the combinations used and the overall penetration level on the system.

TABLE III

Case Scenarios of Wind Dispersion on Two Different Locations

N°	% de combinaison G31 (Low)-G32 (High)	% of combinaison G32 (Low)-G31 (High)	% of Total combination
C0	0%-0%	0%-0%	0%
C1	5%-5%	5%-5%	10%
C2	5%-10%	5%-10%	15%
C3	5%-15%	5%-15%	20%
C4	10%-10%	10%-10%	20%
C5	10%-15%	10%-15%	25%
C6	5%-20%	5%-20%	25%
C7	5%-25%	5%-25%	30%
C8	10%-20%	10%-20%	30%
C9	15%-15%	15%-15%	%30

The results of multiple wind farm location obtained by [5] but with increase the load a 40% and without VSC-MTDC is shown in Table IV, and the results obtained from the simulation where the penetration level of wind farm is low at bus 31 and high at bus 32 and the penetration level of wind farm is low at bus 32 and high at bus 31 by VSC-MTDC is shown in Table V.

TABLE IV

Wind Generation Impact on Active Power Losses and Cost

N°	G10 -Low G24-High	G10-Low G24-High	G24-Low G10-High	G24-Low G10-High
	Cost Value	P Losses	Cost Value	P Losses
C0	1268.5	14.90	1268.5	14.90
C1	1109.2	13.6434	1109.2	13.6085
C2	1039.7	13.4876	1039.8	13.5082
C3	977.0	13.6786	975.1	13.1587
C4	974.7	13.0533	974.7	13.0531
C5	913.9	13.0972	912.0	12.5579
C6	918.3	14.3359	912.6	12.7478
C7	863.2	15.6172	852.2	12.4663
C8	856.8	13.7903	851.3	12.1882
C9	852.8	12.6385	852.8	12.6373

TABLE V

Wind Generation with VSC-MTDC Impact on Active Power Losses and Cost

N°	G31-Low G32-High	G31-Low G32-High	G32-Low G31-High	G32-Low G31-High
	Cost Value	P Losses	Cost Value	P Losses
C0	1268.5	14.90	1268.5	14.90
C1	1202.2	9.067	1202.2	9.067
C2	1152.7	8.116	1152.8	8.082
C3	1109.2	7.972	1108.1	7.429
C4	1107.0	7.370	1107.0	7.370
C5	1029.8	8.072	1052.8	7.052
C6	1.0338	8.660	1.0551	7.188
C7	1.0000	9.921	993.53	7.242
C8	1.0001	8.472	992.19	6.969
C9	994.38	7.462	994.38	7.462

The table IV and V shows generation cost and real power loss for different wind penetration levels and location of wind farm. The generation cost and real power loss have reduced due to the optimal location and mixture combination.

The results obtained from different scenarios give a signal to the utility on what penetration level and location is optimal with respect to active power losses and cost generation.

. Connecting the two wind farms for two cases with and without VSC-MTDC will be a better option in terms reduction in the total costs and power losses for high penetration level (20%, 25%, and 30%). The results obtained for the case of connecting the two wind farms by VSC-MTDC shown better results for the real power loss; in contrary, the results obtained by [5] with increased the load has better value for the cost generation. The best combination is obtained by the combination C8 for the G24 Low and G10 High for two cases, and the voltage of the AC busses in the limit acceptable. Following the installation of large offshore wind farms, the influence of wind energy on the transmission grid has grown.

❖ **Case 2 :** Effect of outage the converter VSC4

In this part, we studied the system of transport of wind energy by VSC-MTDC for the normal case and the case of outage the converter 4, in order to get the change happened on the generation cost, loss and voltage profile.

To perform this simulation, we used the combination C8 (G24 Low and G10-High)

Case 1: before outage of the VSC4
Case 2: after the outage of the VSC4

The detailed operation modes of VSC station are given in Table VI.

TABLE VI

OPERATION MODE OF VSC STATION

VSC stations	$P_{DC}(MW)$	$V_{DC}(KV)$	$Type$	$AC\ bus$
$VSC1$	Slack	± 132	PV	Bus2
$VSC2$	-79.35	± 132	PV	Bus31
$VSC3$	39.68	± 132	PV	Bus5
$VSC4$	-39.68	± 132	PV	Bus32

The results of optimal power flow for combined AC and VSC-MTDC system with connected to wind farms for two cases before and after outage the VSC4 are given in the Table VII, and the power flow in the DC system of two cases as show in Figure 8 and Figure 9.

TABLE VII

Resultants Simulation of DE-OPF for Two Cases

	Case 1	Case 2
$P_{G1}(MW)$	73.01	91.51
$P_{G2}(MW)$	68.68	80.00
$P_{G5}(MW)$	50.00	50.00
$P_{G8}(MW)$	35.00	35.00
$P_{G11}(MW)$	20.94	30.00
$P_{G13}(MW)$	40.00	40.00
$P_{WIND1}(MW)$	79.35	79.35
$P_{WIND2}(MW)$	39.68	00.00
P_{loss} (MW)	6.969	7.276
Cost ($\$/hr$)	992.1985	1108.8

From Table VII, the powers generated by generator 1, 2 and 11 are increased after outage the VSC4, which leds the farm wind 2 to be out-service. The power generated from the wind farm 2 before outage has been compensated by the generators 1, 2 and 11 after outage the VSC4. The total losses and the cost have the values 7.276 MW and 1108.8 $/hr respectively after outage. After the outage of the converter station VSC4, the power output from the VSC1 and VSC3 reduces the power losses and the cost.

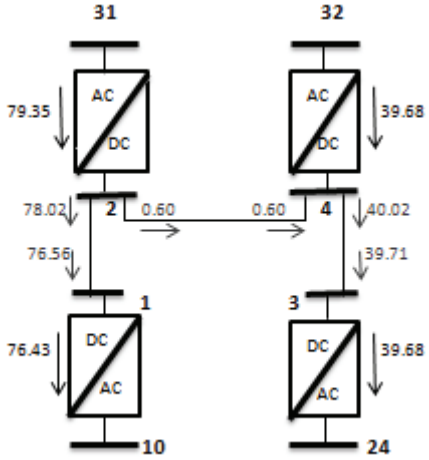

Fig.8 Power flows in the DC bus system before outage

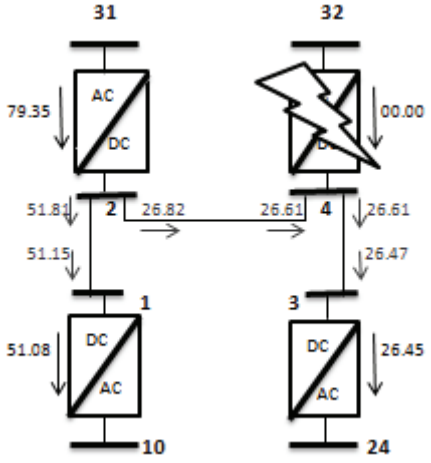

Fig.9 Power flows in the DC bus system after outage

The voltage profile and the power transmitted in all lines in the limits acceptable for the two cases before and after the converter station VSC4 as show in Fig (10.11).

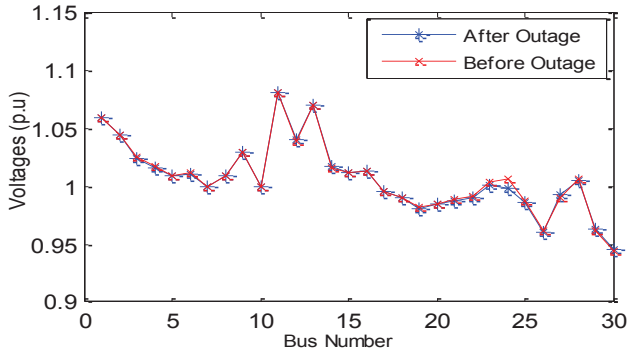

Fig.10 Voltage profile before and after outrage VSC2

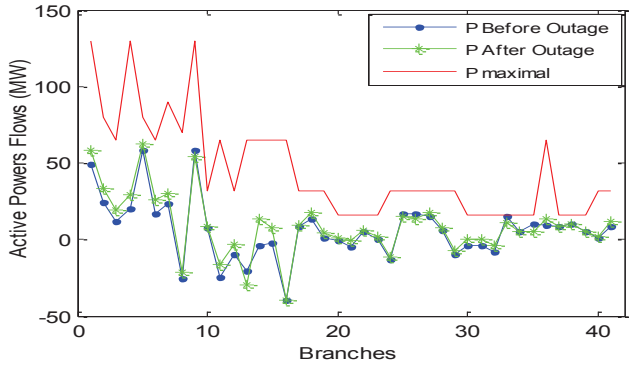

Fig.11 Active powers flow in branch with MTDC before and after outage VSC2

5. CONCLUSION

This paper presented an optimal power flow in presence of Multi-Terminal HVDC Grids with large penetration of wind farm. We studied the impact of integration the huge wind farm with VSC based MTDC on the power system using an evolutionary method which is the differential evolution method. The Simulation results show the best combination for the multiple wind farm location for high penetration level, the optimal power flow for combined AC and multi-terminal HVDC Grids before and after VSC station outages minimize the cost generation, the active power losses and reduces the overflow in the transmission line.

REFERENCES

[1] J. Beerten, R. Belmans, "MatACDC - An Open Source Software Tool for Steady-State Analysis and Operation of HVDC Grids," AC and DC Power Transmission, 11th IET International Conference 2015.

[2] F. Akhter, D.E. Macpherson, G.P. Harrison, W.A. Bukhsh, "DC Voltage Droop Control Implementation in the AC/DC Power Flow Algorithm: Combinational Approach", AC and DC Power Transmission, 11th IET International Conference, 2015.

[3] It's Time to connect—Technical Description of HVDC Light Technology, ABB Group, 2008. [Online]. Available: http://www.abb.com/industries/.

[4] C. Cecati, C. Citro, A. Piccolo, and P. Siano, "Smart Operation of Wind Turbines and Diesel Generators According to Economic Criteria", IEEE Transactions On industrial Electronics, VOL. 58, NO. 10, October 2011, pp.4514-4525.

[5] L. Slimani, T Bouktir, "Application of Differential Evolution Algorithm to Optimal Power Flow with High Wind Energy Penetration," Volume 53, Number 1, 2012.

[6] Storn R., Price K., Differential evolution—a simple and efficient adaptive scheme for global optimization over continuous spaces, in: Technical Report TR-95-012, ICSI, 1995.

[7] J. Cao, Wenjuan Du, Haifeng F. Wang, and S. Q. Bu, "Minimization of Transmission Loss in Meshed AC/DC Grids with VSC-MTDC Networks" IEEE Transactions on Power Systems, Vol. 28, NO. 3, August 2013.

[8] S. S. H. Yazdi, S. H. Fathi, J .M. Monfared, E M. Amiri, "Optimal Operation of Multi terminal HVDC Links Connected to Offshore Wind Farms", 11th International Conference on Electrical Engineering/Electronics, 2014.

[9] W. Feng, Le. A .Tuan, L. B. Tjernberg, A. Mannikoff, A. Bergman "A New Approach for Benefit Evaluation of Multiterminal VSC–HVDC Using A Proposed Mixed AC/DC Optimal Power Flow", IEEE Transactions on Power Delivery, VOL. 29, NO. 1, February 2014.

[10] Beerten, J., Cole, S., Belmans, R. "Generalized steady-state VSC MTDC model for sequential AC/DC power flow algorithms", IEEE Trans. Power Syst., pp. 821–829, 27, 2,2012.

[11] G. Daelemans, "VSC HVDC in meshed networks", Master's thesis, Katholieke Universite it Leuven, Leuven, 2008.

[12] J. Beerten, "MATACDC User's Manual ", [Online].Available:http://www.esat.kuleuven.be/electa/teaching/matacdc/MatACDCManual, 2012.

[13] A. J. Wood and B.F. Wollenberg, "Power Generation, Operation and Control" , 2nd Edition, John Wiley, 1996

[14] Glenn W. Stagg, Ahmed H. El Abiad, "Computer methods in power systems analysis", McGrawHill, 1981

[15] O. Herbadji, L. Slimani and T. Bouktir. "Solving Bi-Objective Optimal Power Flow using Hybrid method of Biogeography-Based Optimization and Differential Evolution Algorithm: A case study of the Algerian Electrical Network", Journel of Electrical Systems: 197-215, 12-1-2016.

[16] R. Storn and K. Price, "Differential Evolution – a simple and efficient adaptive scheme for global Optimization over Continuous Spaces", International Computing Science Institute, Berkley, 1995.

[17] Anne-Katrin Marten, "Mixed AC/DC OPF using Differential Evolution for Global Minima Identification," Englewood Cliffs, NJ: 1989.

[18] Santosh Kumar Moryal, Himmat Singh, " Reactive Power Optimization Using Differential Evolution Algorithm, International Journal of Engineering Trends and Technology (IJETT) , Volume 4 Issue 9- Sep 2013.

[19] Aniruddha Bhattacharya, P.K. Chattopadhyay "Hybrid differential evolution with biogeography based optimization algorithm for solution of economic emission load dispatch problems", Expert Systems with Applications, Vol. 38, pp. 14001–14010, 2011.

[20] Ren Zi-wu Zhu Qiu-guo, "Hybrid Algorithm Based on Biogeography-based Optimization and Differential Evolution for Global Optimization", IEEE 9th Conference on Industrial Electronics and Applications (ICIEA), 2014.

[21] A. K. Qin, V. L. Huang, and P. N. Suganthan "Differential Evolution Algorithm with Strategy Adaptation for Global Numerical Optimization "IEEE Transactions ON Evolutionary Computation, VOL. 13, NO. 2, April 2009.